

Nanostructured SiGe:Sb solid solutions with improved thermoelectric figure of merit

M. V. Dorokhin, P. B. Demina, Yu. M. Kuznetsov, I. V. Erofeeva, A. V. Zdrovevshchev,
M. S. Boldin, E. A. Lantsev, A. A. Popov, E. A. Uskova, V. N. Trushin

Lobachevsky State University of Nizhny Novgorod, Gagarin ave. 23, Nizhniy Novgorod, 603950, Russia
dorokhin@nifti.unn.ru

PACS 72.15.Jf

DOI 10.17586/2220-8054-2020-11-6-680-684

Thermoelectric $\text{Si}_{0.65}\text{Ge}_{0.35}\text{Sb}_\delta$ materials have been fabricated by spark plasma sintering of Ge–Si–Sb powder mixtures. The electronic properties of $\text{Si}_{0.65}\text{Ge}_{0.35}\text{Sb}_\delta$ were found to be dependent on the uniformity of mixing of the components, which in turn is determined by the maximum heating temperature during solid-state sintering. Provided the concentration of donor Sb impurity is optimized the thermoelectric figure of merit for the investigated structures can be as high as 0.63 at 490 °C, the latter value is comparable with world-known analogues obtained for $\text{Si}_{1-x}\text{Ge}_x\text{P}_\delta$.

Keywords: thermoelectric energy converters, spark plasma sintering, doping, germanium-silicon, thermoelectric figure of merit.

Received: 9 September 2020

1. Introduction

The $\text{Si}_{1-x}\text{Ge}_x$ substitutional solid solution is one of the most attractive silicon-based materials for the fabrication of thermoelectric energy converters [1–3]. The latter is due to a high chemical and mechanical stability at elevated temperatures which is some important advantage when concerning the applications in an air atmosphere. Some other advantages of $\text{Si}_{1-x}\text{Ge}_x$ are low toxicity and a high degree of silicon-based technological processes development [4].

The main characterizing parameter of thermoelectric materials is the dimensionless thermoelectric figure of merit (ZT):

$$ZT = \frac{\alpha^2 \sigma}{\chi} T, \quad (1)$$

where χ is the thermal conductivity, σ is electrical conductivity (sometimes resistivity $\rho = 1/\sigma$ can be used instead) and α is the Seebeck coefficient, which can be determined by measuring the thermo-voltage (U_{TE}) and a temperature difference (ΔT) between the “hot” and “cold” edges of the material: $\alpha = -U_{TE}/\Delta T$. As a rule, the parameters in (1) are not independent of each other within one material: with increasing σ , the absolute value of Seebeck coefficient decreases and χ increases [5]. Modern technologies such as nanostructuring provide quasi-independent control of thermoelectric coefficients, which allows one to obtain simultaneously low values of χ with high values of α and σ , and, thus, to increase ZT [2, 3, 5].

In the present paper, we report on the results of the study of $\text{Si}_{0.65}\text{Ge}_{0.35}$ thermoelectric structures fabricated by the spark plasma sintering (SPS) of mixture of Si, Ge and Sb powders. The SPS technique provides unique possibilities for the formation of nanostructured materials and controlling the thermoelectric coefficient as well as the parameters of nanostructuring [6, 7]. The main feature of this work is the use of Sb impurities for fabricating the $\text{Si}_{1-x}\text{Ge}_x$, with n-type conductivity, whereas in the majority of prior papers, As or P impurities are used. The advantages of antimony in comparison with P or As [1–6] are lower toxicity [7, 8], in addition using Sb provides a new technological option for fabricating the n-type material. Although antimony has limited solubility in Ge and Si [9], the use of non-equilibrium fabrication techniques such as SPS allows introduction of the impurity over the solubility limit and achieving the doping concentrations sufficient for obtaining high values of ZT . In this paper, the variation of Sb concentration as well as of the sintering modes has been carried out in order to obtain the increased ZT values.

The top value obtained was as high as $ZT = 0.63$ at 490 °C which is comparable with values characteristic for a “classical” phosphorous or boron doped Ge–Si material [2, 6, 10].

2. Experimental

A series of 5 samples of nanostructured $\text{Si}_{0.65}\text{Ge}_{0.35}\text{Sb}_\delta$ ($\delta = 0.005 - 0.009$) was made for this study. The initial powder to be sintered was fabricated by milling the high-purity Ge, Si and Sb bulk pieces with Fritsch Pulverisette 6 ball mill filled with argon to prevent oxidation. The milling modes (6 hours, 250 RPM) provided the average particle size of ≈ 500 nm. The composition of the material was set by weighing the Ge, Si and Sb pieces and then converting the weight percent to atomic percent.

The sintering was carried out using the DR. Sinter Model SPS-625 spark plasma sintering system. The variable parameters were the Sb concentration (0.5 – 0.9 at.%) and a maximal sintering temperature ($T_s = 1080 - 1180$ °C). The following reasons were taken into account when selecting the sintering modes:

- 1) The lower temperature limit was selected to provide efficient mixing of Ge and Si, whereas upper limit was close to the melting point of the Ge–Si mixture. Since the sintering system used was not designed for liquid-phase sintering, melting of the material would lead to a collapse of the process (because of leaking of the melted material through gaps between the mold, graphite paper, and punches).
- 2) The lower antimony concentration limit of 0.5 at.% was selected to provide sufficiently low conductivity to obtain high enough power factor ($\alpha^2\sigma$). The upper limit of 0.9 at.% of antimony allowed us to prevent the formation of large Sb clusters during sintering [7]. As it has been shown in our earlier work [7] the introduction of 1 at.% of Sb or higher into $\text{Ge}_x\text{Si}_{1-x}$ leads to formation of Sb clusters which is accompanied by the decrease of both conductivity and Seebeck coefficient. This significantly reduces the value of ZT .

The other sintering parameters (pressure of 70 MPa, heating rate of 50 °C/min) were kept constant. The sintering temperature was determined by a pyrometer on the outer wall of the mold with sintered powder, with further conversion to the temperature inside the mold [11]. The technological parameters are presented at Table 1.

TABLE 1. Technological parameters of fabricated Si–Ge samples

Sample	Technological Sb content (δ), at.%	Sintering temperature (T_s), °C
1	0.5	1080±10
2	0.5	1180±10
3	0.7	1150±10
4	0.7	1180±10
5	0.9	1180±10

The sintered ingots of $\text{Si}_{0.65}\text{Ge}_{0.35}\text{Sb}_\delta$ were cut into plates on which phase composition studies using X-ray diffraction (XRD) analysis, as well as measurements of thermoelectric coefficients were performed. The Seebeck coefficient was calculated from simultaneous temperature and thermoelectric voltage measurements using chromel-alumel thermocouples [12]. The resistivity was measured by the standard four-probe method. The thermal conductivity was measured by the stationary heat flux method [13]. The measurements were carried out at temperatures ranging from $T_m = 50 - 490$ °C. The technology for structures fabrication, as well as all measurement techniques, are described in detail in [7, 12].

3. Results and discussion

Figure 1 shows X-ray diffraction spectra of the initial powder (1) and samples (1, 3, 5) fabricated at various temperatures. The lines corresponding to unmixed Ge and Si are present in the diffraction pattern of the initial powder (1). Lines associated with Sb were not resolved due to low concentration.

Sintering of a powder at $T_s = 1080 - 1180$ °C leads to the interaction between the components and to the appearance $\text{Si}_{1-x}\text{Ge}_x$ solid solution associated lines at the spectra (Fig. 1, curves 1, 3, 5). This is accompanied by vanishing the Ge-related lines from the spectra, whereas Si-related lines are preserved and their intensity monotonically decreases with the increase of T_s . The latter is attributed to increase of Si and Ge intermixing with the increase of sintering temperature.

Figure 2 shows the temperature dependence of resistivity. All samples displayed n-type conductivity. For the sample 1, fabricated at the lowest temperature of $T_s = 1080$ °C, the dependence is a semiconductor type, and the resistivity value is the highest among the investigated structures. The $\rho(T_m)$ dependences for the Samples 2–5 (which were fabricated at the elevated temperatures) are similar: all the curves are peak functions with the maximum at 200 – 300 °C and the resistivity values varying slightly in the range of $T_m = 30 - 490$ °C. In the case of the same impurity concentration, a lower value of ρ is characteristic for samples sintered at higher temperatures. An increase in impurity concentration in the range of 0.5 – 0.9 at.% leads to decrease of ρ , which is typical for impurity doping of semiconductors.

The thermal conductivity values measured by stationary heat flux method [14] are presented in Table 2. The values are approximately the same for all nanostructures and lie within the range of 2.5 – 3.75 W/m·K. The latter fact

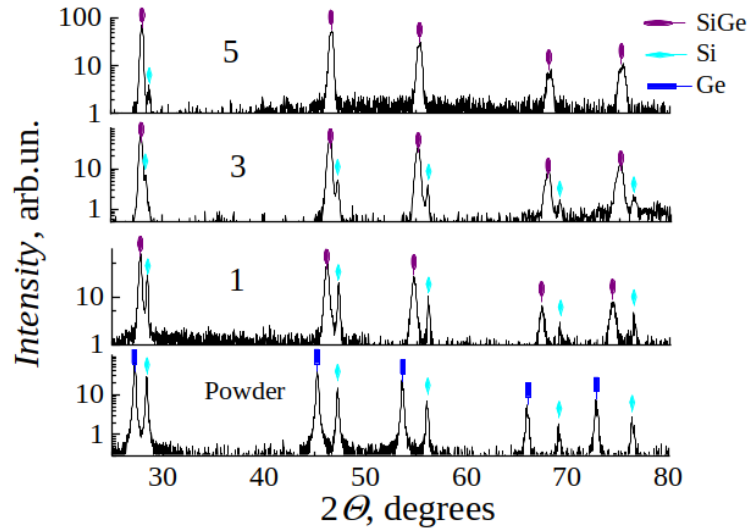


FIG. 1. X-ray diffraction pattern for samples 1, 3, and 5, as well as for the initial powder (Powder). The icons indicate the positions of the peaks for Si, Ge, and a GeSi solid solution

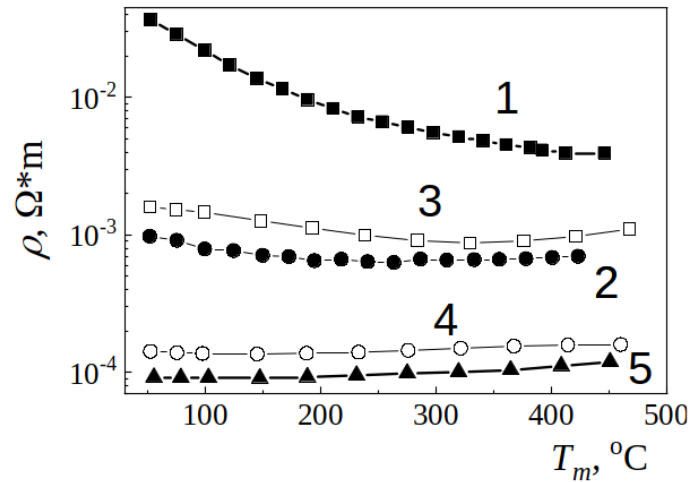


FIG. 2. Temperature dependence of resistivity measured for the samples shown in Table 1. The curve number corresponds to the sample number

can evidence on the similarity of the presented samples both in composition and in grain size. The values of χ in Table 2 are close to the ones obtained for n-Si_{0.60}Ge_{0.40}, highly doped with As or P [14].

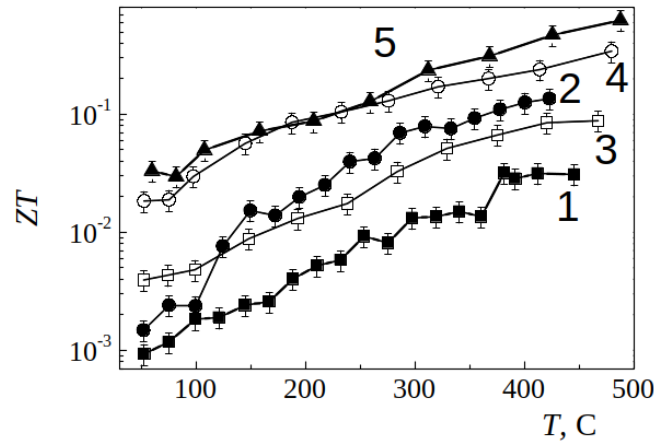
The Seebeck coefficient varies nonmonotonically with varying structural parameters (Table 2), which is believed to be due the α being related with the resistivity. The latter depends not only on the concentration, but also on the homogeneity of the phase composition of the sample.

Figure 3 shows the temperature dependences of ZT , calculated by (1). With the increase of measurement temperature ZT value monotonically increases and the highest values are characteristic of nanostructures with a Sb content of 0.7 to 0.9 at.%. A decrease in impurity concentration, as well as a decrease in sintering temperature, leads to a significant decrease in ZT .

The obtained results can be explained in terms of the phase composition of the samples and the degree of the impurity incorporation into the substitution position of Ge or Si. An insufficient fabrication temperature leads to ineffective mixing of Ge and Si, which is accompanied by the conservation of the silicon phase (this can be seen from the XRD patterns in Fig. 1). The resulting heterogeneity of the Si_{1-x}Ge_x composition leads to modulation of the band gap, thereby causing a slight increase in resistance (compare samples 2 and 3 in Table 2 with the same Sb concentration, but different sintering temperatures). In turn the resistance increase causes a decrease in ZT .

TABLE 2. Thermoelectric parameters of $\text{Si}_{0.65}\text{Ge}_{0.35}\text{Sb}_\delta$ samples. The parameter were measured at $T_m = 450^\circ\text{C}$

Sample	$\rho \times 10^4$, $\Omega\cdot\text{m}$	α , $\mu\text{V}/\text{K}$	χ , $\text{W}/\text{m}\cdot\text{K}$	ZT
1	40 ± 2	410 ± 40	2.5 ± 0.3	0.03 ± 0.006
2	7 ± 0.5	690 ± 40	3.5 ± 0.3	0.14 ± 0.03
3	11 ± 1	644 ± 40	3.2 ± 0.3	0.09 ± 0.02
4	2.0 ± 0.2	490 ± 40	3.75 ± 0.3	0.30 ± 0.06
5	1.2 ± 0.1	490 ± 40	2.73 ± 0.3	0.54 ± 0.1

FIG. 3. Temperature dependences of the thermoelectric figure of merit (ZT) measured for the samples shown in Table 1. The curve number corresponds to the number of the sample

In addition, the incorporation of substitutional impurities into the solid solution substantially depends on the sintering temperature. We believe that the high resistance values of the low-temperature sample 1 are due to the both of the above factors. When sintering the sample with the highest Sb concentration of 0.9 at.% and at a higher temperature, the material with the highest value of ZT is obtained (sample 5, Table 2).

Finally, we should note that the conditions for efficient phase mixing and conditions for efficient Sb incorporation may differ. Indeed, one would need fundamentally nonequilibrium sintering conditions to incorporate the Sb impurity over the solubility level, whereas Ge and Si mixing may occur in the thermal equilibrium. In particular introduction of Sb with the concentration of over 1 at.% in [7] had led to a formation of antimony clusters in the $\text{Si}_{0.65}\text{Ge}_{0.35}$ matrix accompanied with the sharp increase of the resistivity. The poor Ge and Si intermixing also leads to a resistivity increase, as has been shown in the present paper.

The experimental conditions described in section 1 allowed us to achieve both sufficient Ge and Si mixing and Sb impurity incorporation sufficient to obtain the high values of ZT . However, we believe that this combination can still be optimized by further manipulation of the sintering parameters.

4. Conclusion

Thus, the study of the thermoelectric properties of $\text{Si}_{0.65}\text{Ge}_{0.35}$ with Sb impurity has shown that the values of resistivity and thermal conductivity for given impurity concentration are determined mainly by the phase composition of $\text{Si}_{0.65}\text{Ge}_{0.35}$ and the degree of impurity incorporation. The best thermoelectric characteristics were obtained for the structures fabricated at temperatures above 1100°C . The latter value is close to the melting temperature of $\text{Si}_{0.65}\text{Ge}_{0.35}$ solid solution. The top value of $ZT = 0.628$ was obtained at the maximal measurement temperature of 490°C for $\text{Si}_{0.65}\text{Ge}_{0.35}$ with 0.9 at.% of Sb impurity. This value is comparable with the best known phosphorous doped $\text{Si}_{0.8}\text{Ge}_{0.2}$ analogs [2, 6, 10]. As is known, Si-Ge alloys have a unique advantage in using waste heat at a high temperature of

~ 800 – 900 °C. On the other hand, the largest share of waste heat sources is in the range of 300 – 500 °C. Therefore, the operating temperature of approximately 500 °C is also of great interest for practical application.

In conclusion, it was demonstrated for the first time that antimony doping, similarly to phosphorus doping, can be used to obtain the n-type $\text{Si}_{1-x}\text{Ge}_x$ thermoelectric solid solutions.

Acknowledgements

The work was supported by Russian Science Foundation, project no. 17-79-20173, RFBR 20-38-70063, 20-32-90032.

References

- [1] Yu B., Zebarjadi M., Wang H., et.al. Enhancement of thermoelectric properties by modulation-doping in silicon germanium alloy nanocomposites. *Nano Lett.*, 2012, **12**, P. 2077–2082.
- [2] Bathula S., Gahtori B., Jayasimhadri M., et.al. Microstructure and mechanical properties of thermoelectric nanostructured n-type silicon-germanium alloys synthesized employing spark plasma sintering. *Appl. Phys. Lett.*, 2014, **10**, 061902.
- [3] Chen Z.-G., Han G., Yang L., et.al. Nanostructured thermoelectric materials: Current research and future challenge. *Prog. Nat. Sci.: Materials International*, 2012, **22**, P. 535–549.
- [4] Shikari Y., Usami N. Silicon-Germanium (SiGe) nanostructures. Production, properties and application in electronics. *Woodhead publishing limited*, 2011.
- [5] Gayner C., Kar K.K. Recent advances in thermoelectric materials. *Progress Mater. Sci.*, 2016, **83**, P. 330–382.
- [6] Ovsyannikov D.A., Popov M.Y., Buga S.G., et.al. Transport properties of nanocomposite thermoelectric materials based on Si and Ge. *Physics of the Solid State*, 2015, **57**, P. 605–612.
- [7] Dorokhin M.V., Demina P.B., Erofeeva I.V., et.al. In-situ doping of thermoelectric materials based on SiGe solid solutions during their synthesis by the spark plasma sintering technique. *Semiconductors*, 2019, **53**, P. 1158–1163.
- [8] Health N.J. Hazardous substance Fact Sheet. Antimony. URL: <https://web.doh.state.nj.us/rtkhsfs/factsheets.aspx>.
- [9] Olesinski R.W., Abbaschian G.J. The Sb–Si (Antimony-Silicon) system. *Bulletin of Alloy Phase Diagrams*, 1985, **6**, P. 445–448.
- [10] Murugasami R., Vivekanandhan P., Kumaran S., et.al. Simultaneous enhancement in thermoelectric performance and mechanical stability of p-type SiGe alloy doped with Boron prepared by mechanical alloying and spark plasma sintering. *J. Alloys and Comp.*, 2019, **773**, P. 752–761.
- [11] Chuvildeev V.N., Boldin M.S., Dyatlova Y.G., et.al. Comparative study of hot pressing and high-speed electropulse plasma sintering of $\text{Al}_2\text{O}_3/\text{ZrO}_2/\text{Ti}(\text{C},\text{N})$ powders. *Russian Journal of Inorganic Chemistry*, 2018, **60**, P. 987–993.
- [12] Erofeeva I.V., Dorokhin M.V., Zdoroveyshchev A.V., et.al. Production of Si- and Ge-based thermoelectric materials by spark plasma sintering. *Semiconductors*, 2018, **52**, P. 1559–1563.
- [13] Devyatkova E.D., Petrov A.V., Smirnov I.A., Moizhes B.Y. Fused silica as a reference material in measurements of thermal conductivity. *Soviet Phys. Solid State*, 1960, **2**, P. 738–746.
- [14] Schaffler F., Levinshtein M.E., Rumyantsev S.L., Shur M.S. Properties of Advanced Semiconductor Materials GaN, AlN, InN, BN, SiC, SiGe. John Wiley & Sons, Inc., New York, 2001, 188 p.